dard, respectively). It has been argued that values greater than −8 per mil indicate the beginning of an unambiguous C_4 dietary signal (7). A $\delta^{13}C_{en}$ value of −8 per mil assumes a water-stressed, high light C_3 isotopic composition of ∼−22 per mil (due, in part, to an assumed 1.5 per mil enrichment in ^{13}C of Miocene atmospheric CO_2 relative to today) and a fractionation of 14.3 per mil between plant and tooth enamel (7). However, the $\delta^{13}C$ values of terrestrial C_3 plants ($\delta^{13}C_{C3plant}$) range from ∼−33 to −22 per mil, with the majority ranging between −28 and −26 per mil (49). Thus, a $\delta^{13}C_{C3plant}$ value of −22 per mil represents a highly conservative end member. Furthermore, available data support a range of values for the fractionation between mammalian diet and carbonate apatite ($\Delta_{plant-en}$ = 12 to 14.3 per mil) (7, 50). Therefore, with the use of a less conservative approach, a tooth enamel $\delta^{13}C$ value of −8 per mil could constitute a 10 to 30% C_4 influence if one assumes an average $\delta^{13}C_{C3plant}$ = −25 per mil, a $\delta^{13}C_{C4plant}$ = −12 per mil, and maximum and minimum values for $\Delta_{plant-en}$ of 14 and 13 per mil, respectively.

30. T. E. Cerling, Y. Wang, J. Quade, *Nature* **361**, 344 (1993).
31. J. Quade, T. E. Cerling, J. R. Bowman, *ibid.* **342**, 163 (1989).
32. C. Latorre, J. Quade, W. C. McIntosh, *Earth Planet. Sci. Lett.* **146**, 83 (1997).
33. Y. Wang, T. E. Cerling, B. J. MacFadden, *Palaeogeogr. Palaeoclimatol. Palaeoecol.* **107**, 269 (1994).
34. B. J. MacFadden, Y. Wang, T. E. Cerling, F. Anaya, *ibid.*, p. 257.
35. C. France-Lanord and L. A. Derry, *Geochim. Cosmochim. Acta* **58**, 4809 (1994).
36. M. E. Patzkowsky, *Paleobiology* **21**, 440 (1995).
37. P. W. Hattersley, *Oecologia* **57**, 113 (1983); in *Desertified Grasslands: Their Biology and Management*, G. P. Chapman, Ed. (Academic Press, New York, 1992), pp. 181–212.
38. R. L. Bernor *et al.*, in *The Evolution of Western Eurasian Neogene Mammal Faunas*, R. L. Bernor, V. Fahlbusch, H.-W. Mittmann, Eds. (Columbia Univ. Press, New York, 1996), pp. 449–469; S. D. Webb, R. C. Hulbert, W. D. Lambert, in *Paleoclimate and Evolution*, E. S. Vrba, G. H. Denton, T. C. Partridge, L. H. Burckle, Eds. (Yale Univ. Press, New Haven, CT, 1995), pp. 91–108; D. I. Axelrod, *Bot. Rev.* **51**, 163 (1985); E. M. Van Zinderen and J. H. Mercer, *Palaeogeogr. Palaeoclimatol. Palaeoecol.* **56**, 217 (1986); L. J. Flynn and L. L. Jacobs, *ibid.* **38**, 129 (1982).
39. T. E. Cerling and J. Quade, *Chem. Geol.* **84**, 164 (1990); J. Quade, N. Solounias, T. E. Cerling, *Palaeogeogr. Palaeoclimatol. Palaeoecol.* **108**, 41 (1994).
40. D. K. Rea, H. Snoeckx, L. H. Joseph, *Paleoceanography* **13**, 215 (1998).
41. D. K. Rea, *Rev. Geophys.* **32**, 159 (1994).
42. G. J. Retallack, *Palaios* **12**, 380 (1997).
43. W. F. Ruddiman, W. L. Prell, M. E. Raymo, *J. Geophys. Res.* **94**, 18409 (1989); W. F. Ruddiman, J. E. Kutzbach, I. C. Prentice, in *Tectonic Uplift and Climate Change*, W. F. Ruddiman, Ed. (Plenum Press, New York, 1997), pp. 204–235.
44. D. A. Hodell and F. Woodruff, *Paleoceanography* **9**, 405 (1994).
45. D. K. Rea, in *Synthesis of Results from Scientific Drilling in the Indian Ocean* (American Geophysical Union, Washington, DC, 1992), pp. 387–402.
46. T. A. Davies, W. W. Hayes, J. R. Southam, T. R. Worsley, *Science* **197**, 53 (1977).
47. A. Shemesh, R. A. Mortlock, P. N. Froelich, *Paleoceanography* **4**, 221 (1989).
48. G. M. Filippelli and M. L. Delaney, *ibid.* **9**, 643 (1994).
49. P. Deines, in *Handbook of Environmental Isotope Geochemistry*, P. Fritz and J. Fontes, Eds. (Elsevier, Amsterdam, 1980), pp. 329–345.
50. J. A. Lee-Thorp, J. C. Sealy, N. J. van der Merwe, *J. Archaeol. Sci.* **16**, 585 (1989); P. L. Koch, A. K. Behrensmeyer, M. L. Fogel, *Annu. Rep. Dir. Geophys. Lab. Carnegie Inst. Washington* **1990–1991**, 163 (1990–1991).
51. G. Mook, J. C. Bommerson, W. H. Staberman, *Earth Planet Sci. Lett.* **22**, 169 (1974); C. S. Romanek, E. L. Grossman, J. W. Morse, *Geochim. Cosmochim. Acta* **56**, 419 (1992).
52. J. Erez and B. Luz, *Geochim. Cosmochim. Acta* **47**, 1025 (1983).
53. Alkenones were recovered from sediments by Soxhlet extraction in a 2:1 aziotrope of methylene chloride and methanol. The total lipid extracts were separated by silica gel column chromatography into compound classes. Resulting ketone fractions were analyzed by gas chromatography. Shallow-dwelling planktonic foraminifera (*Globogerinoides quadrilobatus*) were selected from the 354- to 420-μm sieved fraction, and the resulting carbon isotopic compositions were used to calculate δd by assuming equilibrium conditions and applying temperature-dependent isotope equations (51). Mixed-layer temperatures were calculated from the $\delta^{18}O$ of *G. quadrilobatus* (52) assuming a value of 0 per mil [standard mean ocean water (SMOW)] for the oxygen isotope value of seawater. $\delta^{18}O = [R_{sa}/R_{std}) - 1] \times 1000$, where R represents the $^{18}O/^{16}O$ abundance ratio and subscripts sa and std represent the sample and SMOW standard, respectively.
54. B. N. Popp, F. Kenig, S. G. Wakeham, E. A. Laws, R. R. Bidigare, *Paleoceanography* **13**, 35 (1998).
55. B. N. Popp *et al.*, in *Reconstructing Ocean History: A Window into the Future*, F. Abrantes and A. Mix, Eds. (Plenum, New York, in press).
56. F. Weiss, *Mar. Chem.* **2**, 203 (1974).
57. Propagation of errors was determined with a Monte Carlo procedure. We assume uncertainties in our method, including the following: $[PO_4^{3-}]$, ±0.1; temperature (degrees Celsius), ±2; salinity, ±1; ε_f, ±1; analytical errors for $\delta_{37:2}$ and $\delta^{13}C_{foram}$ of ±0.5 per mil and ±0.2 per mil, respectively; and an 11% uncertainty about the slope and intercept of the b versus $[PO_4]$ geometric mean regression (representing the 95% confidence interval).
58. Samples for this project were provided by the DSDP/Ocean Drilling Program. This research was funded by grants from NSF and Joint Oceanographic Institutions/U.S. Science Advisory Committee. We would like to thank D. Walizer and G. Montemurro for their invaluable analytical assistance, L. Colorusso for helpful discussions, and P. Koch and J. Eigenbrode for their constructive comments and suggestions.

8 February 1999; accepted 17 June 1999

Hf Isotope Evidence for Pelagic Sediments in the Source of Hawaiian Basalts

J. Blichert-Toft,[1]* F. A. Frey,[2] F. Albarède[1]

Lead, oxygen, and osmium isotopic ratios measured on Hawaiian basalts can be matched with the isotopic ratios inferred for recycled ancient oceanic crust. High-precision hafnium isotopic data for lavas from several Hawaiian volcanoes identify old pelagic sediments in their source. These observations support the recycling hypothesis, whereby the mantle source of ocean island basalts includes ancient subducted oceanic crust. Hyperbolic lead-hafnium isotopic relations among Hawaiian basalts further indicate that upper mantle material is not involved in the production of hot spot basalts.

The apparently fixed position of hot spots on a global scale (*1*) and the constant drift velocity of their volcanoes (*2*) with respect to the underlying asthenosphere suggest that they originate deep in the mantle. The high $^3He/^4He$ ratios of ocean island basalts (OIBs) relative to those of mid-ocean ridge basalts (MORBs) (*3, 4*) reflect a relatively low $(U + Th)/^3He$ ratio in the OIB mantle, which may indicate that the lower mantle is less degassed than the upper mantle (*5*). This interpretation, which has provided a major constraint on models of mantle convection, conflicts with evidence that the source of OIBs is recycled oceanic lithosphere, material expected to be largely degassed. Trace element abundances (*6*) and isotopic ratios of Pb, Nd, and Hf (*7, 8*) indicate that primitive mantle is not the principal source of OIBs. Osmium isotopic measurements suggest that the source of OIBs is enriched in a component that was once extracted from the mantle as a liquid (*9*). Among the shields of Hawaiian volcanoes, the two extreme compositions are typified by the Mauna Kea and Koolau lavas, which fall at the opposite end-points of the Kea and Loa compositional trends, respectively (*10, 11*). The $^{187}Os/^{188}Os$ ratios and $\delta^{18}O$ of Koolau basalts are higher than in MORB, and these high values are characteristic of aged and altered oceanic crust (*9–11*). In contrast, the $\delta^{18}O$ of Mauna Kea basalts is lower than MORB values, possibly reflecting altered lower oceanic crust (*10*).

Oxygen and Os isotopes, however, cannot be used to distinguish between altered basaltic sections of the oceanic crust and the overlying deep-sea sediments (*11*), because it is the magnitudes of the isotopic shifts induced by these two components of the oceanic crust, and not their direction, that are the distinctive features. The recycling of sediments in the source of OIBs is an integral part of the initial formulation of the recycling hypothesis (*12, 13*). Sediments derived from continental detritus have distinctive Nb/U and Ce/Pb ratios compared with these ratios in basalts; however, these ratios in OIBs have been used to argue both for (*14*) and against (*15*) recycled continental ma-

[1]Ecole Normale Supérieure de Lyon, 69364 Lyon Cedex 7, France. [2]Massachusetts Institute of Technology, Cambridge, MA 02139, USA.

*To whom correspondence should be addressed. E-mail: jblicher@ens-lyon.fr

terial in the source of OIBs. The Lu/Hf ratio is a potentially more useful ratio because it can be monitored by $^{176}Hf/^{177}Hf$. The Hf inventory of continental rocks is largely hosted in refractory zircons, a mineral with low (<0.005) Lu/Hf. Because zircons are not generally transported to abyssal plains (*16*), the sedimentary column entering several subduction zones may be dominated by zircon-free, high-Lu/Hf pelagic sediments (*17*).

White *et al.* (*18*) showed that pelagic sediments and ferromanganese nodules have $^{176}Hf/^{177}Hf$ ratios more radiogenic than normal continental crust material. Albarède *et al.* (*19*) demonstrated that the $^{143}Nd/^{144}Nd$ and $^{176}Hf/^{177}Hf$ ratios of ferromanganese nodules, which may record the isotopic properties of fine-grained material settling in the ocean, form a coherent trend, with more radiogenic Hf with respect to a given Nd isotopic composition than normal OIB. Likewise, the Hf isotopic compositions of mud are distinctly more radiogenic than the coarse fractions coexisting in the same detrital sediments (*20*). The position of OIB lavas in a Hf-Nd isotopic correlation plot is therefore potentially diagnostic of the presence or absence of a pelagic component in the OIB source.

Samples from several Hawaiian volcanoes, for which a variety of isotopic compositions are available from the literature, have been analyzed for their Hf isotope compositions (Table 1) with multiple-collector, magnetic-sector, inductively-coupled-plasma mass spectrometry (the VG Plasma 54 in Lyon) after sample dissolution in Savillex vessels and a two-stage column separation procedure (*21*). The Hf isotope results are plotted in the Hf-Nd isotopic correlation diagram in Fig. 1 together with ferromanganese nodules, pelagic sediments, and the mantle-crust array consisting of MORB and OIB that merge with the crust at low ε_{Hf} and low ε_{Nd}. The OIB array (*20*) has a slope of 1.49 ± 0.04 and a positive intercept of $\varepsilon_{Hf} = +2.13 \pm 0.24$ (both values at the 95% confidence level). In contrast, fitting all the Hawaiian basalt measurements yields a slope of 1.00 ± 0.03 with an intercept of $\varepsilon_{Hf} = +5.22 \pm 0.17$ (Fig. 1). When the volcanoes are considered individually (Fig. 2), the Mauna Kea lavas contain the most radiogenic Hf and Nd (although the Haleakala alkali basalt H62-47 is more radiogenic), whereas the Koolau lavas contain the least radiogenic Hf and Nd. Significant individual correlations are found for Haleakala and Koolau with a slope (0.8 with a correlation coefficient R^2 of 0.98 for each of the volcanoes) even shallower than that of the overall Hawaiian trend (Fig. 2). Hawaiian basalts as a group, and Hawaiian volcanoes individually, therefore form arrays that indicate unradiogenic Nd and Hf isotope compositions that plot distinctly above the mantle-crust array, and indicate a component with a long-term, relatively high Lu/Hf, which is typical of pelagic sediments (*16, 20*). In addition to being least radiogenic in ε_{Hf}–ε_{Nd} space, basalts from Koolau volcano also have the highest La/Nb and $^{187}Os/^{188}Os$ ratios and the highest $\delta^{18}O$ values of all the Hawaiian lavas (*9–11, 22*), suggesting that it may contain the largest fraction of pelagic component. The high La/Nb, $^{187}Os/^{188}Os$, and $\delta^{18}O$ were previously used to suggest oceanic crust as a source component for the Koolau lavas (*9–11, 22–24*).

The presence of pelagic sediments in the source of Hawaiian basalts can also be inferred from the ε_{Hf} versus $^{206}Pb/^{204}Pb$ plot (Fig. 3) where the samples define a smooth mixing hyperbola. Although this is an expected trend for mantle-crust mixtures because the end-members have very different Hf/Pb or Os/Pb abundance ratios (*25*), it had not been identified among the Hawaiian basalts. A least square fit of the points was used to determine the position of the asymptotes. Only one ratio per end-member, $^{206}Pb/^{204}Pb$ for Koolau and ε_{Hf} for Kea, can be inferred with precision, the other ratio depending on the Hf/Pb concentration ratios. The ε_{Hf} of the Kea component is about 12.9, lower than modern upper mantle, either asthenospheric or lithospheric; for example, MORB has an ε_{Hf} value of about +20 (*26*).

Table 1. Hf and Nd isotopic compositions for various Hawiian volcanoes.

Sample	$^{176}Hf/^{177}Hf$*	ε_{Hf}†	ε_{Nd}	Source of Nd isotope data
		Loihi volcano		
1801-5	0.283109 ± 5	11.9	5.7	(*42*)
1802-4b	0.283123 ± 3	12.4	6.3	(*42*)
1804-10	0.283106 ± 6	11.8	6.1	(*42*)
1804-21	0.283115 ± 5	12.1	6.0	(*42*)
		Kilauea Hilina volcano		
EK 9-77	0.283116 ± 3	12.2	6.7	(*44*)
EK 20-77	0.283109 ± 3	11.9	6.9	(*44*)
EK 28-77	0.283130 ± 4	12.7	7.1	(*44*)
		Kilauea Puu Oo volcano		
KE30-362 (1985)	0.283112 ± 4	12.0	6.1	(*45*)
1-7-90 (1990)	0.283113 ± 5	12.1	6.2	(*45*)
4-25-94 (1994)	0.283118 ± 4	12.2	6.2	(*45*)
1-10-98 (1998)	0.283112 ± 4	12.0	6.1	(*48*)
		Kilauea volcano		
Kil-1919 (std)	0.283116 ± 4	12.2	6.4	(*49*)
Kil-1919 (std)	0.283116 ± 4	12.2		
BHVO-1 (Kil-1919)	0.283109 ± 4	11.9	6.2	(*12*)
		Kahoolawe volcano		
KW-1	0.283008 ± 4	8.4	3.3	(*43*)
KW-2	0.283014 ± 5	8.6	2.8	(*43*)
KW-5	0.283117 ± 4	12.2	5.7	(*43*)
KW-6	0.283076 ± 6	10.8	4.9	(*43*)
KW-7	0.283095 ± 4	11.4	6.6	(*43*)
KW-14	0.283042 ± 8	9.6	5.5	(*43*)
KW-16	0.283057 ± 3	10.1	5.1	(*43*)
KW-18	0.283040 ± 7	9.5	5.1	(*43*)
KW-19	0.282976 ± 5	7.2	1.8	(*43*)
KW-23	0.283051 ± 5	9.9	5.1	(*43*)
KW-24	0.283044 ± 5	9.6	4.5	(*43*)
KW-25	0.283064 ± 10	10.3	4.1	(*43*)
H-1440	0.283029 ± 5	9.1	4.4	(*43*)
		Haleakala volcano		
HO-9	0.283135 ± 7	12.8		
HO-11	0.283121 ± 5	12.3	7.3	(*41*)
HO-12	0.283106 ± 7	11.8	6.1	(*41*)
HO-17	0.283087 ± 5	11.1	5.7	(*41*)
HO-19	0.283098 ± 5	11.5	6.1	(*41*)
H62-47	0.283180 ± 5	14.4	9.6	(*40*)
		Koolau volcano		
KOO-1	0.282951 ± 10	6.3	2.0	(*23*)
KOO-8	0.282940 ± 7	5.9	1.4	(*23*)
KOO-9	0.282942 ± 6	6.0	1.4	(*23*)
KOO-17A	0.282896 ± 4	4.4	0.2	(*11*)
KOO-17A	0.282903 ± 5	4.6		
KOO-30	0.282910 ± 6	4.9	−0.9	(*23*)
6308	0.283075 ± 6	10.7	6.7	(*24*)

*Uncertainties reported on Hf measured isotope ratios are $2\sigma/\sqrt{n}$ analytical errors in the last decimal place, where n is number of measured ratios. Normalized for mass fractionation to $^{179}Hf/^{177}Hf = 0.7325$. $^{176}Hf/^{177}Hf$ of JMC-475 Hf standard = 0.28216 ± 1. †ε_{Hf} values were calculated with $(^{176}Hf/^{177}Hf)_{CHUR(0)} = 0.282772$.

This confirms the conclusions reached by Lassiter and Hauri (*11*) that upper mantle material is not entrained by the ascending plume (*27*), or that, if it is entrained, it is not melted together with the recycled components. The $^{206}Pb/^{204}Pb$ ratio of the Koolau "sedimentary" component is constrained by the least square mixing hyperbola to a value of about 17.85. Similar but more noisy plots provide values of $^{207}Pb/^{204}Pb$ = 15.43 and $^{208}Pb/^{204}Pb$ = 37.8. As indicated by the concavity of the mixing curve, the Koolau component has a lower Hf/Pb ratio than the Kea component. To evaluate the relative Hf/Pb fractionation between these two components, we assumed $^{206}Pb/^{204}Pb = 19.1$ for Kea and $\varepsilon_{Hf} = +1$ for Koolau (Fig. 3). Using the appropriate equations developed on pages 26 to 28 of (*28*), we infer that the Hf/Pb in the Kea component is 40 times that of the Koolau component. Even if a different set of isotopic compositions is chosen for the end-members, this figure is reliable within a factor of 2 and is consistent with the difference in Hf/Pb ratios between the continental crust (*29*) and the depleted mantle (*30*). Hofmann *et al.* (*6*) emphasized the relatively high abundance of Pb in the crust, and we suggest that the inferred low Hf/Pb in the Koolau component indicates that it contains continental, crust-derived sediments.

What is the age of the continentally derived sediment in the Koolau source? No age constraints can be inferred from the Hf and Nd isotopic data because the process of forming pelagic sediments decouples these isotopic systems (*16, 17, 20*), and with radiogenic ingrowth, pelagic sediments move further away from the mantle array. However, this shift is limited because despite the Lu/Hf ratio being high in some deep-sea clays, it is still commonly lower than chondritic in most subducted sediments. In contrast, the Pb isotopic compositions constrain formation ages independently of knowledge of parent/daughter ratios. Lead isotope data on modern pelagic sediments and nodules have an average $^{206}Pb/^{204}Pb$ of 18.8 and an average $^{207}Pb/^{204}Pb$ of 15.6 (*31–33*). If the Koolau end-member and modern pelagic sediments evolved from a common crustal source, such a difference in isotopic compositions, especially for $^{207}Pb/^{204}Pb$, requires U/Pb fractionation about 3 billion years (Gy) ago, presumably as a result of preferential U removal during subduction. It is improbable that ancient deep-sea clays have been preserved intact for such a long time in the deep mantle. We postulate that, upon subduction, the sedimentary material melted and reacted with the ambient mantle thereby producing the hybrid source of the Koolau end-member (*34*).

The ε_{Hf} versus $^{87}Sr/^{86}Sr$ diagram adds a complementary piece of information (Fig. 4). The individual volcanoes form trends fanning out toward the sedimentary end-member, although only by less than 0.0005 units of $^{87}Sr/^{86}Sr$ at $\varepsilon_{Hf} = +6$, with Koolau containing the most radiogenic Sr. This fanning pattern, which can also be seen in an ε_{Nd} versus $^{87}Sr/^{86}Sr$ plot, may reflect differences in the nature of the sediment involved, its age of deposition, and the extent of Rb/Sr fractionation at subduction zones.

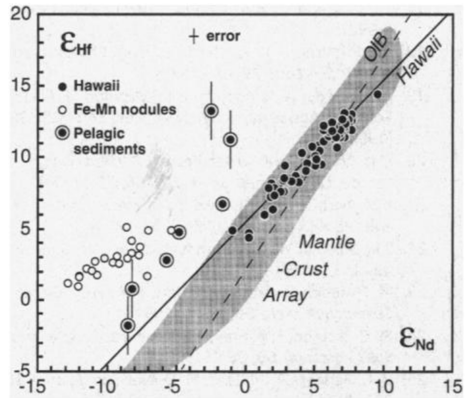

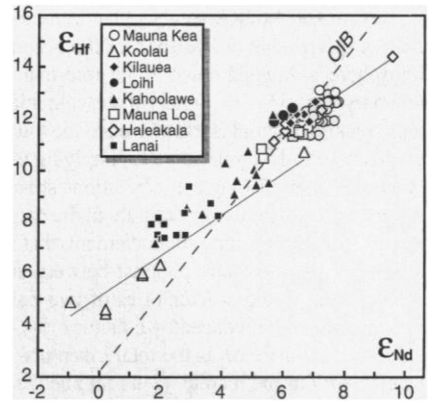

Fig. 1 (Left). Plot of ε_{Hf} versus ε_{Nd} in Hawaiian basalts, including the Hf isotope data for the Hawaiian Scientific Drilling Project core (*39*). Also plotted are Fe-Mn nodules (*19*), pelagic sediments (*20, 33*), and the array of OIBs and MORBs contoured at the 95% confidence level from several hundreds of recent high-precision isotopic data (largely unpublished) and extended toward the crustal field with which it merges. The precision on the parameter ε_{Hf}, which expresses the deviation of the $^{176}Hf/^{177}Hf$ ratio in parts per 10,000 from its value in chondrites, is better than 0.5 unit for the present data. The slope of the Hawaiian basalt trend is shallower (1.00 ± 0.03) than that of the OIB subset (1.49 ± 0.04). It indicates a component, particularly well-represented in Koolau lavas, for which ε_{Hf} and ε_{Nd} plot between the Fe-Mn nodules and pelagic sediments on the one hand and the mantle-crust array on the other hand. Therefore, the Koolau component, which is known to display high $^{187}Os/^{188}Os$ ratios and heavy $\delta^{18}O$ inherited from recycled upper oceanic crust (*9–11*), also contains pelagic sediments. Nd isotope data are from (*11, 12, 23, 24, 40–51*). **Fig. 2 (Right).** Plot of ε_{Hf} versus ε_{Nd} in Hawaiian basalts. As in Fig. 1, but enlarged. The slope of the trends defined by individual volcanoes, such as Koolau and Haleakala, is even shallower (slope = 0.8) than the overall trend of Hawaiian basalts (slope = 1.0). Hf isotope data for Mauna Loa and Mauna Kea are from (*39*), and Hf isotope data for Lanai are from (*51*). Sources of Nd isotope data as in Fig. 1.

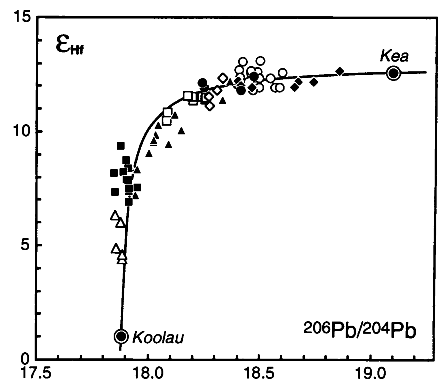

Fig. 3. Plot of ε_{Hf} versus $^{206}Pb/^{204}Pb$ in Hawaiian basalts. The data were fitted by a least square hyperbola (*28*). The "lower crust" Kea component has ε_{Hf} of 12.9, which rules out the participation of asthenospheric or lithospheric material to the melts, whereas the "upper crust" Koolau component has $^{206}Pb/^{204}Pb$ of 17.85. With the hypothetical end-members represented by the dot-symbols ($^{206}Pb/^{204}Pb = 19.1$ for Kea and $\varepsilon_{Hf} = +1$ for Koolau), it can be estimated that the Pb/Hf ratio in the Koolau component is a factor of 40 higher than in the Kea component. Such a high value suggests the existence of sediments in the Koolau component. Legend as in Fig. 2. Sources of Pb isotope data same as for Nd isotope data (see legend of Fig. 1).

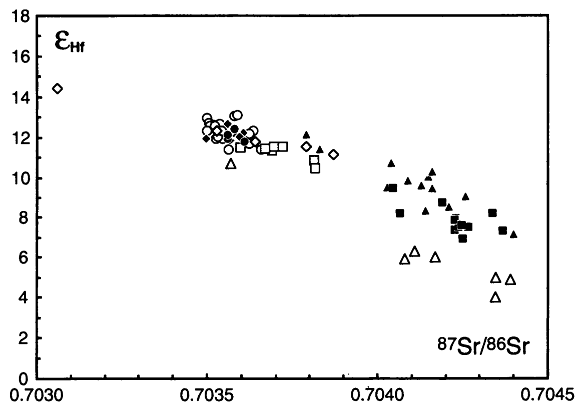

Fig. 4. Plot of ε_{Hf} versus $^{87}Sr/^{86}Sr$ in Hawaiian basalts. The "upper crust" component ($^{87}Sr/^{86}Sr$ > 0.7040) shows a small range of $^{87}Sr/^{86}Sr$ ratios. Such a variability may reflect differences in the nature and age of the sediments or a different extent of Rb/Sr fractionation at subduction zones. Legend as in Fig. 2. Sources of Sr isotope data are the same as for Nd isotope data (see legend of Fig. 1).

It remains unclear how the isotopic signature of a large spectrum of old lithospheric fragments, possibly pelagic sediments and altered basalts and gabbros, can be preserved in the convective mantle and kept isolated from the well-mixed MORB source. Mantle tomography indicates that at least part of the oceanic lithosphere is dragged down to the core-mantle boundary (*35, 36*). At typical plate velocities, upper mantle material is transferred to the lower mantle in 10 to 100 million years, implying that the chemical and isotopic compositions should become homogeneous very rapidly in the entire mantle. The mixing time of an element, that is, the time it takes for any contrast between the chemical and isotopic inventories of two parts of the mantle to be reduced by a factor e, is $f(1 - f)\ M_i/Q_i$, where M_i is the total inventory of the element i in the mantle, Q_i its flux between the two parts of the mantle, and f the fraction of the mantle mass allocated to one of the parts (*37*). For a mass flux equal to the rate of lithosphere subduction (about 300 $km^3\ year^{-1}$), the maximum mixing time of the whole mantle is on the order of 0.4 Gy. Therefore, the lower and the upper mantle should be geochemically indistinguishable. Because OIB and MORB are geochemically distinct, the elemental fluxes Q_i must be reduced and the mixing time of radiogenic isotopes increased so that heterogeneity between the OIB and MORB reservoirs is preserved. Mixing times can be increased by the delamination of the oceanic crust and its storage at the core-mantle boundary (*13, 38*). They may also be selectively increased for different elements by the extraction of continental crust material and by the hydrous stripping of the lithophile elements from the subducting slabs into the ambient mantle without substantial reduction of the total mass of the lithosphere that penetrates into the lower mantle (*37*). Such a process calls for an overall depleted deep mantle with streaks of lithospheric residues altered by subduction zone processes (such as those invoked for the U/Pb fractionation in the source of the Koolau component), but still fertile enough to produce OIBs.

References and Notes

1. J. B. Minster, T. H. Jordan, P. Molnar, E. Haines, *Geophys. J. R. Astron. Soc.* **36**, 541 (1974).
2. J. T. Wilson, *Can. J. Phys.* **41**, 863 (1963).
3. I. Kaneoka and N. Takaoka, *Science* **208**, 1366 (1980).
4. M. D. Kurz, W. J. Jenkins, S. R. Hart, D. Clague, *Earth Planet. Sci. Lett.* **66**, 388 (1983).
5. C. J. Allègre, A. W. Hofmann, R. K. O'Nions, *Geophys. Res. Lett.* **23**, 3555 (1996).
6. A. W. Hofmann, K. P. Jochum, M. Seufert, W. M. White, *Earth Planet. Sci. Lett.* **79**, 33 (1986).
7. C. J. Allègre, *ibid.* **5**, 261 (1969).
8. J. Blichert-Toft and F. Albarède, *ibid.* **148**, 243 (1997).
9. E. H. Hauri and S. R. Hart, *ibid.* **114**, 353 (1993).
10. J. M. Eiler, K. A. Farley, J. W. Valley, A. W. Hofmann, E. M. Stolper, *ibid.* **144**, 453 (1996).
11. J. C. Lassiter and E. H. Hauri, *ibid.* **164**, 483 (1998).
12. W. M. White and A. W. Hofmann, *Nature* **296**, 821 (1982).
13. A. W. Hofmann and W. M. White, *Earth Planet. Sci. Lett.* **57**, 421 (1982).
14. K. W. W. Sims and D. J. DePaolo, *Geochim. Cosmochim. Acta* **61**, 765 (1997).
15. A. W. Hofmann, *Nature* **385**, 219 (1997).
16. P. J. Patchett, W. M. White, H. Feldmann, S. Kielinczuk, A. W. Hofmann, *Earth Planet. Sci. Lett.* **69**, 365 (1984).
17. T. Plank and C. H. Langmuir, *Chem. Geol.* **145**, 325 (1998).
18. W. M. White, J. Patchett, D. Ben Othman, *Earth Planet. Sci. Lett.* **79**, 46 (1986).
19. F. Albarède, A. Simonetti, J. D. Vervoort, J. Blichert-Toft, W. Abouchami, *Geophys. Res. Lett.* **25**, 3895 (1998).
20. J. D. Vervoort, P. J. Patchett, J. Blichert-Toft, F. Albarède, *Earth Planet. Sci. Lett.* **168**, 79 (1999).
21. J. Blichert-Toft, C. Chauvel, F. Albarède, *Contrib. Mineral. Petrol.* **127**, 248 (1997).
22. S.-s. Sun and W. F. McDonough, *Geol. Soc. Spec. Pub.* **42**, 313 (1989).
23. M. F. Roden, T. Trull, S. R. Hart, F. A. Frey, *Geochim. Cosmochim. Acta* **58**, 1431 (1994).
24. M. C. Jackson, F. A. Frey, M. O. Garcia, R. A. Wilmoth, *Bull. Volcanol.* **60**, 381 (1999).
25. V. C. Bennett, T. M. Esat, M. D. Norman, *Nature* **381**, 221 (1996).
26. P. J. Patchett and M. Tatsumoto, *Geophys. Res. Lett.* **7**, 1077 (1980).
27. C. G. Farnetani and M. A. Richards, *Earth Planet. Sci. Lett.* **136**, 251 (1996).
28. F. Albarède, *Introduction to Geochemical Modeling* (Cambridge Univ. Press, Cambridge, 1995).
29. R. L. Rudnick and D. M. Fountain, *Rev. Geophys.* **33**, 267 (1995).
30. S. B. Jacobsen, W. M. White, A. Zindler, http://www-ep.es.llnl.gov/germ/ reservoirs/depleted-mantle.html
31. D. Ben Othman, W. M. White, J. Patchett, *Earth Planet. Sci. Lett.* **94**, 1 (1989).
32. W. Abouchami, S. L. Goldstein, S. J. G. Galer, A. Eisenhauer, A. Mangini, *Geochim. Cosmochim. Acta* **61**, 3957 (1997).
33. L. V. Godfrey *et al.*, *Earth Planet. Sci. Lett.* **151**, 91 (1997).
34. J. Blichert-Toft, F. Albarède, J. Kornprobst, *Science* **283**, 1303 (1999).
35. R. van der Hilst, R. Engdahl, W. Spakman, G. Nolet, *Nature* **353**, 733 (1991).
36. S. P. Grand, *J. Geophys. Res.* **99**, 11591 (1994).
37. F. Albarède, *Chem. Geol.* **145**, 413 (1998).
38. U. R. Christensen and A. W. Hofmann, *J. Geophys. Res.* **99**, 19867 (1994).
39. J. Blichert-Toft and F. Albarède, *Geophys. Res. Lett.* **26**, 935 (1999).
40. C.-Y. Chen, F. A. Frey, M. O. Garcia, *Contrib. Mineral. Petrol.* **105**, 197 (1990).
41. ______, G. B. Dalrymple, S. R. Hart, *ibid.* **106**, 183 (1991).
42. M. O. Garcia, B. A. Jorgenson, J. J. Mahoney, *J. Geophys. Res.* **98**, 537 (1993).
43. W. P. Leeman, D. C. Gerlach, M. O. Garcia, H. B. West, *Contrib. Mineral. Petrol.* **116**, 62 (1994).
44. C.-Y. Chen, F. A. Frey, J. M. Rhodes, R. M. Easton, in *Earth Processes: Reading the Isotopic Code*, A. Basu and S. Hart, Eds. (American Geophysical Union, Washington, DC, 1996), vol. 95, pp. 161–181.
45. M. O. Garcia, J. M. Rhodes, F. A. Trusdell, A. J. Pietruszka, *Bull. Volcanol.* **58**, 359 (1996).
46. E. H. Hauri, J. C. Lassiter, D. J. DePaolo, *J. Geophys. Res.* **101**, 11793 (1996).
47. J. C. Lassiter, D. J. DePaolo, M. Tatsumoto, *ibid.*, p. 11769.
48. M. O. Garcia, A. J. Pietruszka, J. M. Rhodes, K. Swanson, in preparation.
49. A. J. Pietruszka and M. O. Garcia, *J. Petrol.* **40**, 1321 (1999).
50. W. Abouchami, unpublished data on Lanai.
51. J. Blichert-Toft, unpublished data.

52. We thank W. Abouchami for allowing us to use her unpublished Sr, Nd, and Pb isotope data for Lanai; P. Télouk for maintaining the Plasma 54; M. Garcia and B. Leeman for providing samples for this study; M. Garcia for comments on an earlier draft of this manuscript; and two anonymous reviewers for helpful comments. Funding by the Institut National des Sciences de l'Univers, through the program Dynamique des Transferts Terrestres, is gratefully acknowledged.

9 April 1999; accepted 24 June 1999

Molecular Identification of a Eukaryotic, Stretch-Activated Nonselective Cation Channel

Makoto Kanzaki,[1] Masahiro Nagasawa,[1] Itaru Kojima,[1] Chikara Sato,[2] Keiji Naruse,[3] Masahiro Sokabe,[3] Hidetoshi Iida[4]*

Calcium-permeable, stretch-activated nonselective cation (SA Cat) channels mediate cellular responses to mechanical stimuli. However, genes encoding such channels have not been identified in eukaryotes. The yeast *MID1* gene product (Mid1) is required for calcium influx in the yeast *Saccharomyces cerevisiae*. Functional expression of Mid1 in Chinese hamster ovary cells conferred sensitivity to mechanical stress that resulted in increases in both calcium conductance and the concentration of cytosolic free calcium. These increases were dependent on the presence of extracellular calcium and were reduced by gadolinium, a blocker of SA Cat channels. Single-channel analyses with cell-attached patches revealed that Mid1 acts as a calcium-permeable, cation-selective stretch-activated channel with a conductance of 32 picosiemens at 150 millimolar cesium chloride in the pipette. Thus, Mid1 appears to be a eukaryotic, SA Cat channel.

SA Cat channels are suggested to act as mechanotransducers in various biological functions including touch sensation, hearing, and maintenance of cardiovascular tone in animals, detection of touch and gravity in plants, and sensing of osmotic changes in microorganisms (*1*). However, genes or cDNAs encoding eukaryotic SA Cat channels have not been identified, and thus, the molecular mechanism of mechanotransduction in eukaryotic cells is poorly under-